Self-Supporting Nanopore Membranes with Controlled Pore Size and Shape

Zhe-Xue Lu, Arya Namboodiri, and Maryanne M. Collinson*

Department of Chemistry, Virginia Commonwealth University, Richmond, Virginia 23284-2006

ARTICLE

ABSTRACT Self-supporting membranes containing either isolated or organized arrays of nanosized pores have been prepared using a nonlithographic approach by coupling sol—gel processing, thin film preparation, and templating. Specifically, polystyrene latex spheres were doped into a hybrid sol prepared from tetraethoxysilane and dimethyldiethoxysilane and the resultant sol spin cast on a sacrificial support. Upon removal of the template and the sacrificial support, the self-supporting nanopore membranes were transferred to glass for characterization by atomic force microscopy and scanning electron microscopy. Through variations in the thickness of the membranes and the size of the polystyrene latex spheres, the geometry (cylinder-like to asymmetric-like) and the dimensions of the nanopores were altered. Pores with diameters that range from 35 to 2100 nm, aspect ratios (defined as the top pore diameter divided by the bottom pore diameter) from 1—4, and depths (effective film thickness) from 50 to 1500 nms have been prepared using templates that range in diameter from 100 to 3100 nm. The method described employs "wet-chemistry", is highly versatile, and is easily amenable to modification by utilizing templates of different sizes and geometries to create stable membranes with different pore geometries and sizes that can be used as platforms for nanofiltration and/or chemical sensors.

KEYWORDS: nanopore membranes · asymmetric nanopores · sol—gel chemistry · self-supporting membranes · templating

Self-supporting membranes that contain single nanopores or arrays of nanopores have attracted considerable attention because of their potential applications in the controlled growth of nanostructures, nanofiltration devices, bioseparations, and biosensing.[1–3] Long before man walked on earth, nature had succeeded in the creation of "nano"-filtration membranes, most notably the α-hemolysin channel.[4,5] In contrast to biologically based nanopores, "synthetic" mimics have potential advantages of being less fragile, more stable, easily tailored, better able to withstand harsher conditions, and thus more applicable to commercial nanofiltration or sensing devices. These "designer" materials have enormous potential in clinical and diagnostic applications, chemical sensors, separation science, chemical delivery, and catalysis.[1–3]

A number of excellent examples of membranes that contain nanosized pores exist in the literature, perhaps the most popular being the porous alumina membranes and the track-etched membranes popularized by the Martin group.[1,2] More recently, considerable efforts have been directed toward tailoring the geometry of the nanopore in track-etched membranes from cylindrical to conical,[5–10] studying ionic transport in these asymmetric pores,[11–15] and using them as sensing elements to detect various analytes including proteins,[16] porphyrins,[17] and DNA.[18] Conical-shaped pores, where the top diameter of the pore is larger than its bottom, have a number of advantages including enhanced transport properties, lower resistance, and improved sensor performance.[7,16,17] In addition to these studies, other efforts have been directed toward the fabrication of self-supporting films of nanometer thickness that contain nanosized pores[19–22] as well as supported materials that contain nanochannels and nanowells, such as those formed on conducting surfaces, in polymers, silicon, and in glass.[23–29]

Herein, we describe a simple, reliable, nonlithographic approach to create self-supporting membranes that contain single asymmetric nanosized pores or localized arrays of asymmetric nanosized pores by coupling template based strategies,[30,31] thin film processing,[32] and sol—gel polymerization.[33] The method described provides a means to easily tailor the thickness of the self-supporting membranes from nanometers to micrometers, manipulate the density of nanosized pores, and alter the diameter of the nanosized pores and their corresponding aspect ratio (defined as the pore diameter on the top of the membrane to that on the bottom). Furthermore, the membranes are easily amendable to chemical modification and thus have promising

*Address correspondence to mmcollinson@vcu.edu.

Received for review January 1, 2008 and accepted April 02, 2008.

Published online April 30, 2008.
10.1021/nn8000017 CCC: $40.75

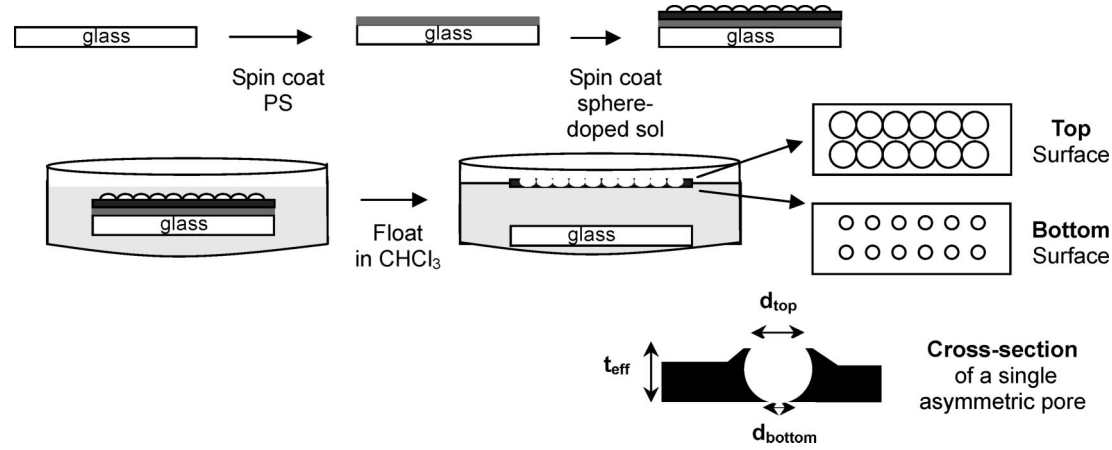

Scheme 1. Preparation of self-supported membranes containing asymmetric nanopores.

applications in the areas of filtration, chemical delivery, and chemical sensing.

RESULTS AND DISCUSSION

Sol−gel processing provides an important and valuable means to form thin films[32,34] on insulating and conducting surfaces and in some less typical cases, self-supporting membranes.[35−38] In previous work,[23] we showed how sol−gel processing can be merged with template based processing to provide a way to create a two-dimensional ordered array of pores (*e.g.*, nanowells) in a thin, insulating film coated on a conducting surface (an electrode). Specifically, polystyrene latex spheres were doped into a silica sol, which was then spin coated on a glassy carbon electrode. The latex spheres were then dissolved in chloroform leaving behind hemispherical cavities in the silica thin film on glassy carbon, which were used to electrochemically grow nanostructures from the bottom up.[23] In this work, we show that under the appropriate circumstances, this same type of approach can be used to create *self-supporting* membranes of varying thickness that contain either single or localized arrays of nanosized asymmetric pores with varying sizes and aspect ratios. It is important to note that in addition to the nanosized pores directly introduced into the membrane upon removal of the spherical templates, the silica framework has associated with it some micro- and mesoporosity, which is difficult to measure because of the small amount of material present. In the discussion below, the term "pore" refers to the pores directly introduced into the membrane when the template (latex sphere) is removed.

Membrane Preparation. One promising method to form self-supporting membranes involves spin coating the appropriate membrane components (in this study, a sphere-doped silica sol) on a polymer coated glass slide.[35−39] By dissolving the underlying polymer support in an appropriate solvent, the membrane detaches and floats to the surface while the glass substrate falls to the bottom. The self-supporting membrane can then be transferred onto a suitable substrate for subsequent characterization. A simple cartoon of this process is shown in Scheme 1. In this study, polystyrene (PS) was chosen as the underlying polymer because it easily dissolves in chloroform simultaneously with the template (polystyrene latex spheres) but not the silica membrane.

The pore that remains in the membrane when the template (latex sphere) is removed will typically be asymmetric in that its diameter will be larger on the top of the membrane compared to that on the bottom. The diameter of the pore on the top side of the membrane (d_{top}) will be a function of the diameter of the sphere (template) and the effective film thickness of the film (t_{eff}, defined as the thickness of the film as measured from the pile-up of silica around the sphere to the bottom of the membrane, see later). The diameter of the pore on the bottom side of the membrane (d_{bottom}) will depend on the surface area of the sphere in contact with the underlying surface (polystyrene film). When the underlying polystyrene surface and the polystyrene latex sphere are removed, this "contact" area becomes exposed, thus defining the dimensions of the base of the pore. The diameter of the bottom pore will largely be dependent on the diameter of

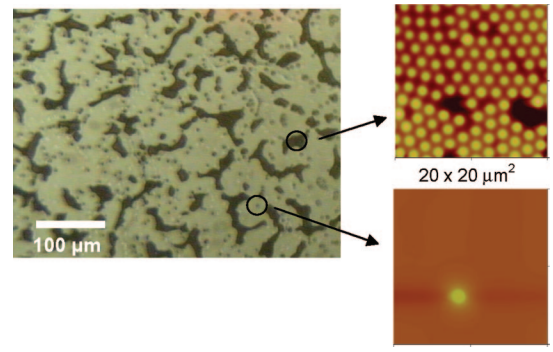

Figure 1. Optical image and corresponding AFM images (20 µm × 20 µm) of 2-µm diameter spheres in a silica membrane before chloroform treatment. Z axis scale in AFM images: 1000 nm (top image of ensemble) and 10000 nm (bottom image of single sphere).

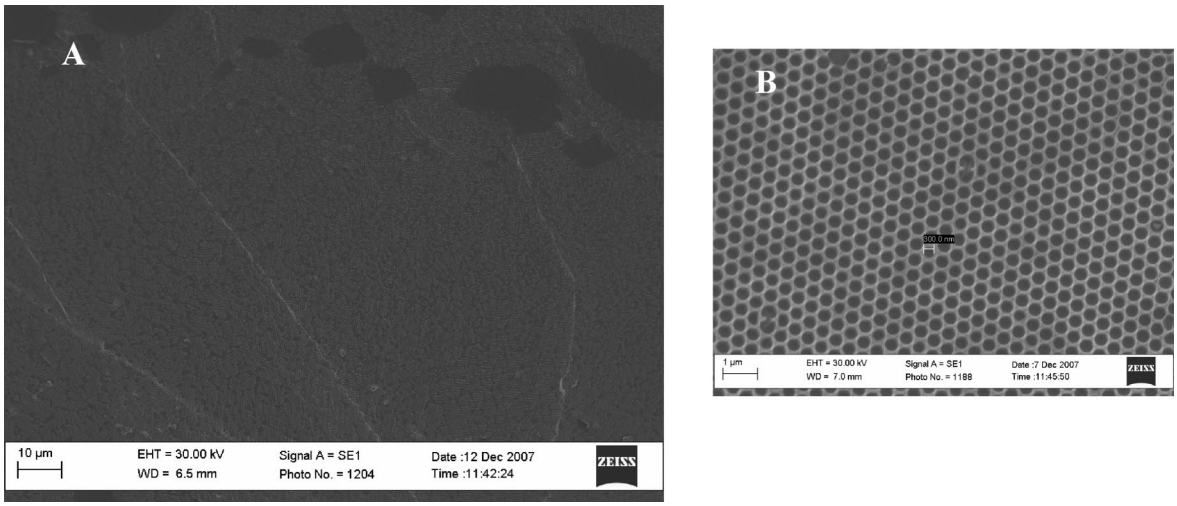

Figure 2. SEM images of a hybrid membrane prepared from the 440-nm diameter spheres after treatment in chloroform. Panel B represents an expanded view of the top of the membrane showing pores that are *ca*. 300 nm in diameter.

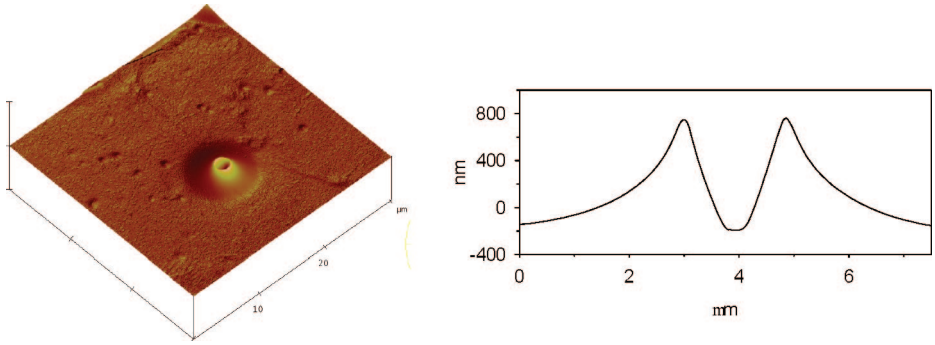

Figure 3. 3D AFM image (30 μm × 30 μm; *Z*-axis: 5000 nm) of a single pore in a hybrid membrane prepared from a 2-μm diameter sphere. The plot shows the corresponding sectional of the single pore.

the sphere but not the film thickness. The aspect ratio, defined as the ratio of d_{top} to d_{bottom}, will depend on the size of the sphere, the effective film thickness, and the surface area of the sphere in contact with the underlying surface. This ratio can easily be modified and tuned by changing one or more of these variables.

To be of use in any meaningful investigation, it is critical that the self-supporting membrane be stable and not easily broken into tiny pieces. While sol−gel chemistry provides a versatile means to prepare thin films,[32,34] particularly when coated on a suitable substrate, the thin films are fragile, especially when they are prepared from traditional precursors such as tetraethoxysilane (TEOS). To overcome this disadvantage as well as to provide a means to create thicker films and membranes, organoalkoxysilanes have been combined with the traditional tetrafunctional silanes (*i.e.*, TEOS) to prepare a hybrid composite material.[40,41] Alternatively, organic polymers can be added to the sol to prepare more flexible membranes.[37,38]

In this investigation, a number of organoalkoxysilanes were evaluated as a means to create thicker, more flexible thin films that can be detached from a surface without fracturing including methytrimethoxysilane, phenyltrimethoxysilane, and dimethyldiethoxysilane (DMDEOS).[39] Other variables that needed to be considered included the ratio of the tetrafunctional cross-linker (*i.e.*, TEOS) to the organoalkoxysilane, the composite sol's aging time before spin coating, and the membranes drying time and environment. Films that are not properly cross-linked (condensed) owing to an inadequate drying time, temperature, environment, or not prepared from a sufficiently aged (condensed) sol will easily fragment when placed in solvent. These variables were first optimized using 3-μm diameter spheres as the template. The most promising results were obtained using a 5:2 mixture of TEOS/DMDEOS, a one day aging period, and a two day film drying period under moderate humidity. The hybrid membranes *without spheres* prepared under these conditions are *ca.* 50−200 nm thick as measured by profilometry. The effective film thickness, t_{eff}, of the nanopore membranes ranges from approximately 50 to 1500 nm.

Membrane Characterization. The membranes transferred to glass were either imaged using AFM or SEM. In both cases, similar images were obtained. A representative optical image of the hybrid film containing 2.0 μm spheres on plasma-treated PS coated glass can be seen in Figure 1. The dark areas in the optical image represent areas where the spheres are densely packed as

TABLE 1. Top/Bottom Pore Diameter with Different Size Microsphere Templates[a]

	diameter of microsphere templates					
	3.1 μm	2.0 μm	990nm	440nm	210nm	95nm
top pore size (d_{top}), nm	2060 ± 100	1130 ± 30	458 ± 18	200 ± 14	78 ± 9	41 ± 9
bottom pore size (d_{bottom}), nm	516 ± 40	365 ± 38	185 ± 32	138 ± 15	76 ± 13	35 ± 9
aspect ratio (d_{top}/d_{bottom})	4.0	3.1	2.5	1.4	1.0	1.2

[a]The sol used is the original aged sol, with the exception of the 210 and 95 nm diameter spheres where the sol was diluted with ethanol (40 μL of sol to 60 μL of ethanol (210 nm spheres) and 50 μL of sol to 50 μL of ethanol (95 nm spheres)) and spin coated at 8000 rpm. Error represents standard deviations from $N = 9-12$ pores.

can be seen in the corresponding AFM image. Also present, are areas where there are no spheres and areas where a single sphere can be found (see corresponding AFM image). In some investigations, it may be useful to focus on a single pore formed from a single sphere whereas in other investigations it may be useful to focus on an ensemble of pores formed from a closely packed array of spheres. The films described herein provide a means to look at either a single pore or an ensemble of closely spaced pores.

When the sphere-doped membrane is placed in chloroform, the membrane detaches from the underlying polystyrene/glass support and floats to the surface and the latex spheres dissolve leaving behind nanosized pores in the hybrid membrane. Figure 2A shows a SEM image of a large area of the top surface of a membrane prepared using 440 nm diameter spheres captured on glass. Both "single" pores and localized arrays of pores can be seen in these large scale images. A SEM image of an "ordered" region in this film is shown in Figure 2B, depicting pores that have a top diameter of *ca.* 300 nm. With the spin coating method we are using now, ordered regions with a maximum size of approximately 10 μm × 10 μm are typically obtained. By relying on other methods to order the spheres on the polymer coated glass slide besides spin coating,[42] it should be possible to obtain membranes where the entire arrangement of the template induced pores is closely packed, thus providing materials with the highest possible density of asymmetric pores.

A representative AFM image of *a single pore* in a self-supporting membrane (transferred on glass for AFM imaging) prepared from a 2-μm diameter sphere is shown in Figure 3. In a 3-D AFM plot, the pore looks like a volcano as the sol initially wets the sphere and then pulls away, exposing the top of the particle and building up around the sides.[23,43] The single pore that is produced upon dissolving the template is more clearly shown in the sectional image. Theoretically, the shape of the pore will mimic the shape of the bottom half of the template—a hemisphere. But because the AFM tip can not contact (and thus, properly image) the inner walls of the hemispherical pore, the geometry of the "actual" pore will look more "bowl" shaped (*i.e.*, see cartoon in Scheme 1) compared to that seen in Figure 3. In most cases, d_{top} will be greater than d_{bottom}, giving rise to the term "asymmetric" pore.

Pore Size Variations. Once film preparation conditions have been optimized, membranes with different long-range order, film thickness, pore sizes, and aspect ratios were prepared by varying the size of sphere and the viscosity of the sol. Spheres with a diameter from 100 nm to 3 μm were used in this study. However, it should be possible to create even smaller pores by utilizing spheres that are in the 20−100 nm size, which can also be purchased commercially. Figure 4 shows AFM images of the top and bottom surfaces of three typical membranes formed by templating with different size microspheres (2000, 990, and 440 nm).

The average pore diameters at the top and bottom of the membranes are summarized in Table 1. As seen in Figure 4 and Table 1, the top and bottom pore diameter is dependent on the diameter of the microsphere templates used. The larger the diameter of the sphere, the larger the top and bottom diameters of the pores in the membranes. Likewise, the aspect ratio, defined as the top diameter divided by the bottom diameter, can be changed by changing the diameter of the template. This value also depends on the effective film thickness of the membrane. It is possible that the bottom diameter is larger than what may be theoretically expected, particularly for the pores prepared from the smaller spheres, because the film surrounding the base of the pore is very thin, potentially making it more fragile and possibly more easily broken during detachment.

TABLE 2. Top/Bottom Pore Diameter in Films of Varying Thicknesses Prepared by Diluting the Original Sol with Ethanol Prior To Spin Coating[a]

	dilution of original sol with ethanol (total volume = 100 μL)				
dilution factor	0%	20%	40%	50%	60%
top pore size (d_{top}), nm	200 ± 14	231 ± 14	257 ± 15	313 ± 22	369 ± 17
bottom pore size (d_{bottom}), nm	138 ± 15	128 ± 13	136 ± 13	128 ± 13	137 ± 14
aspect ratio	1.4	1.8	1.9	2.4	2.7

[a]Template: 440 nm diameter polystyrene microspheres. Error represents standard deviations from $N = 9-12$ pores. Effective film thickness varies from *ca.* 350 to 250 nm.

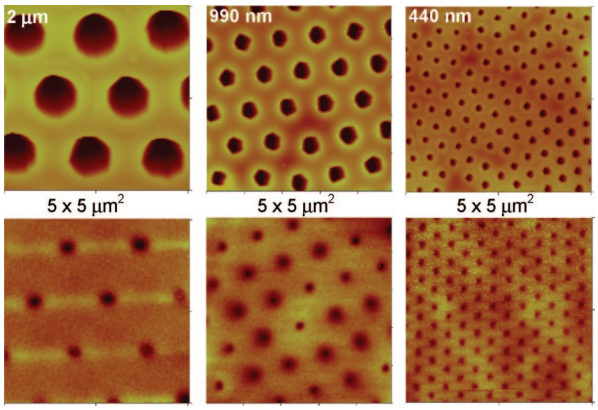

Figure 4. AFM images of membranes templated with different size microspheres (2 μm, 990 nm, and 440 nm). (Top row) Top side of membrane. (Bottom row) Corresponding bottom side of membrane. *Z*-scale in top side images: 2000 nm (2 μm spheres) and 400 nm (990 and 440 nm). *Z*-scale in bottom side images: 50 nm.

Another powerful means to change the top diameter of the pore, and thus the aspect ratio of the pores, is to change the thickness of the film by changing the viscosity of the sol. In this study, the 440 and 95 nm diameter microspheres were used as the model templates and the original sol was diluted with ethanol to change its viscosity to produce self-supporting silica membranes with different thickness (see Scheme 2).

Figure 5 shows AFM images of three typical membranes of different thicknesses using the 440 nm diameter templates. The pore size of both top/bottom sides of the membranes are summarized in Table 2. The top diameter of the pore clearly depends on the effective film thickness (which varies by a factor of *ca*. 1.5), but the bottom diameter does not. The maximum aspect ratio that can be obtained is the diameter of the sphere divided by the d_{bottom} (determined by the surface contact with the surface). By optimizing the effective film thickness, asymmetric pores with maximum aspect ratios can be obtained. When 40 μL of sol was diluted with 60 μL ethanol, for example, pores with the largest aspect ratio (~3) were obtained using the 440 nm diameter spheres as templates: top, 369 nm; bottom, 137 nm. Similar results were observed with the 95 nm diameter spheres as shown in Figure 6. When the sol is diluted with 50, 70, and 80 μL of ethanol, the top diameter of the pore varied and was 41 ± 9, 62 ± 12, and 80 ± 10 nm, respectively. The bottom diameter was 35 ± 9 nm.

Changes in the film thickness and changes in the diameter of the template also provide a means to change the "geometry" of the pore from one where the aspect ratio is near 1 (cylinder-like) to one where it can be greater than 4 (asymmetric-like). The 95 nm diameter spheres, for example, give rise to a cylinder-like geometry (aspect ratio near 1) when the sol is diluted 50:50 with ethanol and an asymmetric-like geometry when diluted 20:80 sol/ethanol (aspect ratio 2.3). Likewise, at the given film thicknesses, the 210 nm diameter spheres have nearly identical bottom and top diameter (Table 1) with an aspect ratio near 1 (cylinder-like) while the 3-μm diameter spheres give rise to the most asymmetric shape with bottom and top diameters differing by 4.

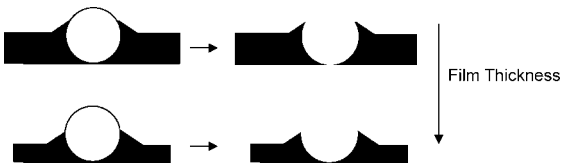

Scheme 2. Simplified diagram depicting how film thickness influences pore diameters and aspect ratios.

CONCLUSION

In summary, large, flexible, self-supporting silica membranes that contain asymmetric pores can be obtained by combining sol−gel technology with thin film processing with template based strategies using nano- to micrometer-sized polystyrene latex spheres as the template. The density of nanopores in the membrane can range from a single isolated pore to arrays of closely spaced pores. The shape of the nanopore as well as its aspect ratio can be easily modified through changes in the size of the template and through dilution of the sol. While this work has focused on the fabrication of membranes with aspect ratios between 1 and 4, with pore sizes ranging from 2100 to 35 nm, it should be possible to extend these ranges *via* further manipulation of template diameter, template shape, and film thickness. Since the membranes were made using the sol−gel process, it is possible to trap molecules in the pores that will be able to react with analytes passing through the nanopore. Silica is

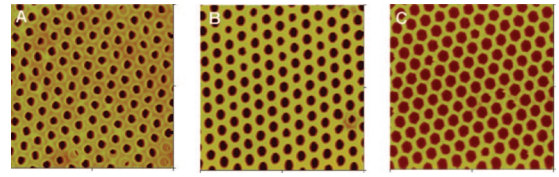

Figure 5. AFM images of the top side of membranes prepared with 440 nm diameter spheres: (A) dilution of 60 μL the original sol with 40 μL of ethanol; (B) dilution of 50 μL the original sol with 50 μL of ethanol; (C) dilution of 40 μL the original sol with 60 μL of ethanol. Image: 5 μm × 5 μm. *Z* scale: 400 nm (A), 400 nm (B), and 800 nm (C).

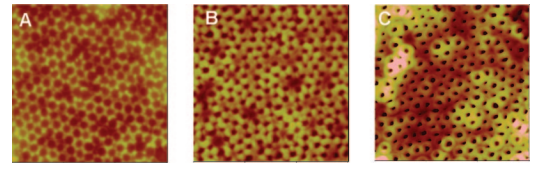

Figure 6. AFM images (1.5 μm × 1.5 μm) of the top side of membranes prepared with 95 nm diameter spheres: (A) dilution of 20 μL the original sol with 80 μL of ethanol; (B) dilution of 30 μL the original sol with 70 μL of ethanol; (C) dilution of 50 μL the original sol with 50 μL of ethanol. *Z* scale: 100 nm.

also easily amenable to surface modification allowing the inside of the pore as well as the pore mouth and tip to be modified to influence transport and enhance selectivity. The membranes are also relatively thin (0.05 to 1.5 μm) in comparison to the more traditionally studied track-etched conical polymer membranes containing nanopores (typically 10 μm) thus potentially improving transport rates. These thin self-supporting membranes thus have promising applications in the areas of bioseparations, filtration, chemical delivery, and chemical sensing. Future work is being directed toward these applications.

EXPERIMENTAL SECTION

Reagents. Tetraethoxysilane (TEOS, 99%) and dimethyldiethoxysilane (DMDEOS, 97%) were purchased from Aldrich. Chloroform, methylene chloride, and hydrochloric acid were purchased from Fisher Scientific. Polystyrene (MW ≈ 45K) was purchased from Aldrich. Aqueous suspensions of polystyrene microspheres with diameters ranging from 0.1 to 3 μm were obtained from Interfacial Dynamics Corp. (Portland, OR) (8.2 wt/v %, surfactant free, sulfated). Water was purified with a Millipore water system.

Preparation of Self-Supporting Nanopore Membranes. Glass microscope slides were cut into 1.5 cm × 1.5 cm squares and cleaned by successive sonication in soap, ethanol, and water. These slides were then spin coated with polystyrene (1 g dissolved in 8 mL of methylene chloride) at 2000 rpm for 20 s using a commercial spin coater. The film thickness of the polystyrene layer was about 1.5 μm as measured *via* profilometry (KIA-Tencor). The polystyrene coated slides were dried for one day (42% humidity), plasma cleaned for 10 s (Harrick Plasma Cleaner, low power) to make the surface more hydrophilic, and then spin coated with sol. The original sols with DMDEOS/TEOS molar ratio of 2:5 were prepared by mixing the appropriate amount of TEOS (100 μL), DMDEOS (32 μL), 200 μL of ethanol, and 30 μL of 0.1 M hydrochloric acid followed by stirring for 30 min, and then aged for one day at room temperature. Polystyrene microspheres (0.095, 0.21, 0.44, 0.99, 2.0 and 3.1 μm diameter) were sonicated 5−10 min before use. The aged (1 day) silica sol (100 μL) was then added to a spheres suspension (100 μL) in a ratio of 1:1. For the experiments using a diluted sol, the total sol volume was still kept at 100 μL, dilution was done by mixing 100, 80, 60, 50, 40, 30, and 20 μL of the original aged sol with 0, 20, 40, 50, 60, 70 and 80 μL of ethanol, respectively. The sphere-doped silica sols were then spin cast on the polystyrene-coated glass substrate at *ca.* 3000 rpm (for the 440 nm and larger spheres) or 8000 rpm (for the 95 and 210 nm spheres) for 25 s. The thin membranes supported on polystyrene coated glass were allowed to dry for 2 days at *ca.* 40−45% humidity at room temperature.

To detach the film from the substrate as well as to remove the template (polystyrene latex spheres) to create the asymmetric pores, the glass slide was placed in a glass Petri dish and chloroform was slowly added until the membrane/glass slide was completely immersed. The membrane immediately floated to the top, and after one hour, it was transferred onto a clean glass substrate. The "bottom" side of the membrane proved to be more difficult to "capture" for subsequent imaging. The method that proved best was to capture the top surface of the membrane on glass, invert it, and put it in contact with a second hydrophobic glass substrate (silanized in 1% octyltrimethoxysilane in methanol overnight) to form a "sandwich". The bottom side of the "hydrophobic" membrane preferentially sticks to the hydrophobic glass. Upon slow addition of water, the "hydrophilic" top glass floats away leaving the membrane with its bottom side facing up on the hydrophobic glass substrate for drying and subsequent imaging. The membranes were dried overnight in a desiccator and imaged using an atomic force microscope (AFM, Digital Instruments, Nanoscope IIIa, Tapping mode) with silicon nitride tips (Nanoscience Instruments) or a scanning electron microscope (SEM, Zeiss, EVO 50 XVP). Prior to imaging on the SEM, a thin layer of gold was deposited on the membranes.

Acknowledgment. Support of this work by the National Science Foundation (Grant CHE-0618220) and the VCU Honors Summer Undergraduate Research Program are gratefully acknowledged. The Higher Education Equipment Trust Fund provided by the Commonwealth of Virginia is also gratefully acknowledged for funds used to purchase the profilometer. Mike Shultz is thanked for his help with the acquisition of the SEM images.

REFERENCES AND NOTES

1. Martin, C. R. Membrane-Based Synthesis of Nanomaterials. *Chem. Mater.* **1996**, *8*, 1739–1746.
2. Baker, L. A.; Jin, P.; Martin, C. R. Biomaterials and Biotechnologies Based on Nanotube Membranes. *Crit. Rev. Solid State Mater. Sci.* **2005**, *30*, 183–205.
3. Bayley, H.; Martin, C. R. Resistive-Pulse Sensing-from Microbes to Molecules. *Chem. Rev.* **2000**, *100*, 2575–2594.
4. Bayley, H.; Cremer, P. S. Stochastic Sensors Inspired by Biology. *Nature* **2001**, *413*, 226–230.
5. Harrell, C. C.; Siwy, Z. S.; Martin, C. R. Conical Nanopore Membranes: Controlling the Nanopore Shape. *Small* **2006**, *2*, 194–198.
6. Scopece, P.; Baker, L. A.; Ugo, P.; Martin, C. R. Conical Nanopore Membranes: Solvent Shaping of Nanopores. *Nanotechnology* **2006**, *17*, 3951–3956.
7. Li, N. C.; Yu, S. F.; Harrell, C. C.; Martin, C. R. Conical Nanopore Membranes. Preparation and Transport Properties. *Anal. Chem.* **2004**, *76*, 2025–2030.
8. Lebedev, K.; Mafe, S.; Stroeve, P. Modeling Electrochemical Deposition inside Nanotubes to Obtain Metal-Semiconductor Multiscale Nanocables or Conical Nanopores. *J. Phys. Chem. B* **2005**, *109*, 14523–14528.
9. Ramirez, P.; Mafe, S.; Alcaraz, A.; Cervera, J. Modeling of pH-Switchable Ion Transport and Selectivity in Nanopore Membranes with Fixed Charges. *J. Phys. Chem. B* **2003**, *107*, 13178–13187.
10. Ramirez, P.; Mafe, S.; Aguilella, V. M.; Alcaraz, A. Synthetic Nanopores with Fixed Charges: An Electrodiffusion Model for Ionic Transport. *Phys. Rev. E* **2003**, *68*, 011910-1.
11. Vlassiouk, I.; Siwy, Z. S. Nanofluidic Diode. *Nano Lett.* **2007**, *7*, 552–556.
12. Siwy, Z. S. Ion-Current Rectification in Nanopores and Nanotubes with Broken Symmetry. *Adv. Funct. Mater.* **2006**, *16*, 735–746.
13. Cervera, J.; Schiedt, B.; Neumann, R.; Mafe, S.; Ramirez, P. Ionic Conduction, Rectification, and Selectivity in Single Conical Nanopores. *J. Chem. Phys.* **2006**, *124*, 104706-1.
14. Ramirez, P.; Gomez, V.; Cervera, J.; Schiedt, B.; Mafe, S. Ion Transport and Selectivity in Nanopores with Spatially Inhomogeneous Fixed Charge Distributions. *J. Chem. Phys.* **2007**, *126*, 194703-1.
15. Cervera, J.; Alcaraz, A.; Schiedt, B.; Neumann, R.; Ramirez, P. Asymmetric Selectivity of Synthetic Conical Nanopores Probed by Reversal Potential Measurements. *J. Phys. Chem. C* **2007**, *111*, 12265–12273.
16. Siwy, Z.; Trofin, L.; Kohli, P.; Baker, L. A.; Trautmann, C.; Martin, C. R. Protein Biosensors Based on Biofunctionalized Conical Gold Nanotubes. *J. Am. Chem. Soc.* **2005**, *127*, 5000–5001.
17. Heins, E. A.; Siwy, Z. S.; Baker, L. A.; Martin, C. R. Detecting Single Porphyrin Molecules in a Conically Shaped Synthetic Nanopore. *Nano Lett.* **2005**, *5*, 1824–1829.
18. Harrell, C. C.; Choi, Y.; Horne, L. P.; Baker, L. A.; Siwy, Z. S.; Martin, C. R. Resistive-Pulse DNA Detection with a Conical Nanopore Sensor. *Langmuir* **2006**, *22*, 10837–10843.

19. Smoukov, S. K.; Bishop, K. J. M.; Campbell, C. J.; Grzybowski, B. A. Freestanding Three-Dimensional Copper Foils Prepared by Electroless Deposition on Micropatterned Gels. *Adv. Mater.* **2005**, *17*, 751.
20. Peng, X. S.; Jin, J.; Ericsson, E. M.; Ichinose, I. General Method for Ultrathin Free-Standing Films of Nanofibrous Composite Materials. *J. Am. Chem. Soc.* **2007**, *129*, 8625–8633.
21. Fujikawa, S.; Muto, E.; Kunitake, T. Embedding of Individual Ferritin Molecules in Large, Self-Supporting Silica Nanofilms. *Langmuir* **2007**, *23*, 4629–4633.
22. Jiang, C. Y.; Markutsya, S.; Pikus, Y.; Tsukruk, V. V. Freely Suspended Nanocomposite Membranes as Highly Sensitive Sensors. *Nat. Mater.* **2004**, *3*, 721–728.
23. Kanungo, M.; Deepa, P. N.; Collinson, M. M. Template Directed Formation of Hemispherical Cavities of Varying Depth and Diameter in a Silicate Matrix Prepared by the Sol-Gel Process. *Chem. Mater.* **2004**, *16*, 5535–5541.
24. Lanyon, Y. H.; De Marzi, G.; Watson, Y. E.; Quinn, A. J.; Gleeson, J. P.; Redmond, G.; Arrigan, D. W. M. Fabrication of Nanopore Array Electrodes by Focused Ion Beam Milling. *Anal. Chem.* **2007**, *79*, 3048–3055.
25. Lee, H.; Park, J.; Kim, J.; Jung, H.; Kawai, T. Well-Oriented Nanowell Array Metrics for Integrated Digital Nanobiosensors. *Appl. Phys. Lett.* **2006**, *89*, 113901-1.
26. Kang, M. C.; Yu, S. F.; Li, N. C.; Martin, C. R. Nanowell-Array Surfaces Prepared by Argon Plasma Etching through a Nanopore Alumina Mask. *Langmuir* **2005**, *21*, 8429–8438.
27. Yang, S. Y.; Ryu, I.; Kim, H. Y.; Kim, J. K.; Jang, S. K.; Russell, T. P. Nanoporous Membranes with Ultrahigh Selectivity and Flux for the Filtration of Viruses. *Adv. Mater.* **2006**, *18*, 709.
28. Zhang, B.; Galusha, J.; Shiozawa, P. G.; Wang, G. L.; Bergren, A. J.; Jones, R. M.; White, R. J.; Ervin, E. N.; Cauley, C. C.; White, H. S. Bench-Top Method for Fabricating Glass-Sealed Nanodisk Electrodes, Glass Nanopore Electrodes, and Glass Nanopore Membranes of Controlled Size. *Anal. Chem.* **2007**, *79*, 4778–4787.
29. Letant, S. E.; van Buuren, T. W.; Terminello, L. J. Nanochannel Arrays on Silicon Platforms by Electrochemistry. *Nano Lett.* **2004**, *4*, 1705–1707.
30. Raman, N. K.; Anderson, M. T.; Brinker, C. J. Template-Based Approaches to the Preparation of Amorphous, Nanoporous Silicas. *Chem. Mater.* **1996**, *8*, 1682–1701.
31. Huczko, A. Template-Based Synthesis of Nanomaterials. *Appl. Phys. A: Mater. Sci. Process.* **2000**, *70*, 365–376.
32. Brinker, C. J.; Hurd, A. J.; Schunk, P. R.; Frye, G. C.; Ashley, C. S. Review of Sol-Gel Thin Film Formation. *J. Non-Cryst. Solids* **1992**, *147−148*, 424–436.
33. Brinker, J.; Scherer, G., *Sol-Gel Science;* Academic Press: New York, 1990.
34. Brinker, C. J.; Frye, G. C.; Hurd, A. J.; Ashley, C. S. Fundamentals of Sol-Gel Dip Coating. *Thin Solid Films* **1991**, *201*, 97–108.
35. Hashizume, M.; Kunitake, T. Preparation of Self-Supporting Ultrathin Films of Titania by Spin Coating. *Langmuir* **2003**, *19*, 10172–10178.
36. Hashizume, M.; Kunitake, T. Preparations of Self-Supporting Nanofilms of Metal Oxides by Casting Processes. *Soft Matter* **2006**, *2*, 135–140.
37. Vendamme, R.; Ohzono, T.; Nakao, A.; Shimomura, M.; Kunitake, T. Synthesis and Micromechanical Properties of Flexible, Self-Supporting Polymer-SiO_2 Nanofilms. *Langmuir* **2007**, *23*, 2792–2799.
38. Vendamme, R.; Onoue, S. Y.; Nakao, A.; Kunitake, T. Robust Free-Standing Nanomembranes of Organic/Inorganic Interpenetrating Networks. *Nat. Mater.* **2006**, *5*, 494–501.
39. Cao, B.; Zhu, C. S. Sol-Gel Derived Self-Supporting Film. *J. Non-Cryst. Solids* **1999**, *246*, 34–38.
40. Collinson, M. M. Recent Trends in Analytical Applications of Organically Modified Silicate Materials. *TrAC, Trends Anal. Chem.* **2002**, *21*, 30–38.
41. Schubert, U.; Husing, N.; Lorenz, A. Hybrid Inorganic-Organic Materials by Sol-Gel Processing of Organofunctional Metal Alkoxides. *Chem. Mater.* **1995**, *7*, 2010–2027.
42. Xia, Y.; Gates, B.; Yin, Y.; Lu, Y. Monodispersed Colloidal Spheres: Old Materials with New Applications. *Adv. Mater.* **2000**, *12*, 693–713.
43. Khramov, A. N.; Munos, J.; Collinson, M. M. Preparation and Characterization of Macroporous Silicate Films. *Langmuir* **2001**, *17*, 8112–8117.